Astronomy & Astrophysics manuscript no. mc18
April 4, 2013

Probing Cosmic Rays in Nearby Giant Molecular Clouds with the Fermi Large Area Telescope

Rui-zhi Yang[1,2,4], Emma de Oña Wilhelmi[2], and Felix Aharonian[2,3]

[1] Key Laboratory of Dark Matter and Space Astronomy, Purple Mountain Observatory, Chinese Academy of Sciences, Nanjing, 210008, China
[2] Max-Planck-Institut für Kernphysik, P.O. Box 103980, 69029 Heidelberg, Germany
[3] Dublin Institute for Advanced Studies, 31 Fitzwilliam Place, Dublin 2, Ireland
[4] Graduate University of Chinese Academy of Sciences, Beijing, 100012, China

Received ; accepted

ABSTRACT

We report the results of our study on the energy spectra and absolute fluxes of cosmic rays (CRs) in the Local Galaxy based on three-year gamma-ray observations of ten nearby giant molecular clouds (GMCs) belongs to the Gould Belt, with the Fermi Large Area Telescope (LAT). The gamma-ray signals obtained with high statistical significance allow the determination of gamma-ray spectra above 300 MeV with adequate precision for extraction of the energy distributions of CRs in these clouds. Remarkably, both the derived spectral indices and the absolute fluxes of CR protons in the energy interval $10-100$ GeV are in good agreement with the recent direct measurements of local CRs by the PAMELA experiment. This is a strong evidence for a quite homogeneous distribution of CRs, at least within several hundred parsecs of the Local Galaxy. Combined with the well established energy-dependent time of escape of CRs from the Galaxy, $\tau(E) \propto E^{-\delta}$ with $\delta \approx 0.5-0.6$, the measured spectrum implies a CRs spectral index of the (acceleration) source of $\approx E^{-2.3}$. At low energies, the spectra of gamma-rays appear to vary from one cloud to another. This implies spatial variations of the energy spectra of CR below 10 GeV which at such low energies could be naturally explained by the impact of the propagation effects as well as by the contribution of CR locally accelerated inside the clouds.

Key words. Gamma rays: ISM, ISM: clouds, cosmic rays

1. Introduction

The current paradigm of cosmic rays (CR) postulates that the bulk of the CR flux up to the so-called *knee* around 10^{15} eV, is linked to galactic sources, presumably to supernova remnants (see e. g. Drury 2012 for a recent review). Also, it is also believed that, because of the effective mixture of CRs during their propagation in the interstellar magnetic fields, the CR density locally measured in the Earth's neighbourhood should correctly describe the average density of CRs throughout the galactic disk, which can be treated as the level of the *sea* of galactic CRs. Small variations of CRs on large (kpc) scales do not, however, exclude significant variations on smaller scales, in particular in the proximity of young CRs accelerators. Therefore it is not obvious that the locally measured component of CRs can be taken as undisputed representative of the whole galactic population of relativistic particles. In particular, it is possible that the flux of local CRs might be dominated by the contribution of a few nearby sources. On the other hand, because of the solar modulation effects (Adriani et al. 2013), the low energy part of the CR flux, typically below 10 GeV, is strongly distorted, thus the direct measurements contain large uncertainties concerning the level of the *sea* of galactic CRs at low energies. This energy band determines the total luminosity of our Galaxy in CRs and it is crucial for the understanding of several important issues related to the physics of the interstellar medium, e.g. the relative contribution of CRs to the overall pressure in the interstellar medium compared to the magnetic fields and the turbulent and thermal pressure of the gas. The interstellar chemistry through the heating and ionisation of the interstellar gas is another important issue related to low energy CRs.

The density of CRs in different parts of galaxy can be uniquely probed at GeV and hopefully also TeV energies through observations of gamma-rays from massive molecular clouds (Aharonian 2001; Casanova et al. 2010; Pedaletti et al. 2013). The realisation of the method requires detailed spectroscopic measurements of a large number of individual giant molecular clouds (GMCs) with known distances, d, and masses, M. The precision of the method is limited by uncertainties in the ratio of the parameter M/d^2 and by the accuracy in the derivation of the spectral shape of CRs, which depends on the correct identification of the dominant radiation mechanisms and on the accuracy of gamma-ray measurements. The possible presence of potential local accelerators (Montmerle 1979) that can contaminate the CRs *sea* should be also taken into consideration when selecting the GMCs.

Amongst the best candidates for such studies are GMCs linked to the star formation complexes of Gould Belt (Aharonian 2001). These massive clouds ($M \geq 10^5 M_\odot$) are located close-by ($d<500$ pc) and they are usually located offset of the Galactic plane (Perrot & Grenier 2003), where the emission of the large diffuse CRs emission would prevent a clear discrimination of the gamma-ray emission associated to clouds at low latitudes. Their location and size make

Table 1. Properties of the GMCs analysed on LAT data

#	Region	Mass [10^5 $M_\odot$]	Distance [pc]	l [°]	b [°]	M/d^2 [(10^5 $M_\odot$/kpc^2)]	Angular size [arcdeg^2]
1	ρ Oph	0.3	165	356°	18°	11.0	68
2	Hercules	0.16	470	45°	9°	0.72	18
3	Orion B	1.0	500	205°	-14°	4.0	22
4	Orion A	1.3	500	213°	-18°	5.2	28
5	Mon R2	1.2	830	214°	-12°	1.7	19
6	Taurus	0.3	140	170°	-16°	15.3	101
7	R CrA	0.03	150	0.5°	-18°	1.3	8
8	Chamaeleon	0.16	215	300°	-16°	1.3	22
9	Perseus OB2	0.6	350	158°	-20°	4.9	27
10	Aquila	1.5	200	26°	2°	37.5	92

them suitable targets for the Fermi LAT satellite (Atwood et al. 2009).

Recently Neronov et al. (2012) reported the results obtained from their analysis and interpretation of Fermi LAT observations of a number of GMCs associated to the Gould Belt. In the reduction of data they used the so-called aperture photometry method[1]. They claimed evidence of similarity of the energy spectra from different clouds. Therefore to derive a global CR spectrum with good statistics they combine the data from different observed clouds. Doing that they conclude that the mean CR spectrum can be described by a steep power-law with an index 3.0 ± 0.2, with a low energy break at 9 ± 3 GeV. However, due to complex gamma-ray morphology of these objects, expected due to inhomogeneous spatial distribution of the molecular gas, and (potentially) also CRs, the chosen method of determination of energy spectra from these extended objects might lead to misleading conclusions, especially at low energies. The Fermi team has also investigated a few representative GMCs (Ackermann et al. 2012a; Achermann et al. 2012). They used the gamma-ray data to determine the calibration ratio between the CO intensity and the column density (Dame et al. 1987; Grenier et al. 2005), a priori assuming that the CR spectra in different parts of the galactic plane are described by similar spectral shape and flux of the locally measured CRs.

Given the importance of these results regarding the origin of galactic CRs, we conducted an independent study on a cloud-by-cloud basis, based on a different approach of derivation of the energy spectra of gamma-rays. Namely, in our analysis we used the *likelihood* method which has been developed and recommended for spectral studies by the Fermi LAT collaboration[2].

The Gould Belt consists of a concentration of stars forming a ring titled towards the galactic disk by ≈20°. Several of these clusters are identified as active regions of star formation (e. g. Marraco & Rydgren 1981, Hillenbrand 1997, Shimajiri et al. 2011). Their location offset the galactic plane (where the diffuse gamma-ray emission is enhanced) and their proximity to Earth make them suitable candidates for the study CR interactions with matter. Note, however, that active star forming regions can contribute substantially to the acceleration of particles and thus enhance the CR density inside these clouds. If so, this could introduce large uncertainties in the estimate of the flux of galactic CRs and their energy spectrum based on gamma-ray observations of these *active clouds*. On the other hand, the opposite cannot be excluded, i.e. a deficit in the gamma-ray flux compared to the minimum flux expected from GMCs due to interactions of the galactic CRs with the ambient gas. At low energies this could be a quite natural consequence of propagation effects which might prevent the free entrance of CRs into the complex of young stars that surround the clouds, and/or penetration of the particles deep into the dense cores of the clouds, where the bulk emission of gamma-rays could be produced (Aharonian 2001). For high energy protons, typically above 10 GeV, the impact of propagation effects is dramatically reduced, thus a detection of significant deficit in high energy gamma-rays (produced via π^0-decay), even from a single cloud, would require a revision of the level of the *sea* of galactic CRs (Aharonian 2001).

The gamma-ray studies at energies above several hundred MeVs have other advantages when compared to lower energies. First, the degradation of the LAT angular resolution at low energies introduces non-negligible uncertainties in the energy spectrum and flux of of gamma-rays from the clouds. Secondly, while at high energies the contribution to the gamma-ray emission via other channels (bremsstrahlung and inverse Compton scattering of electrons) is not expected to be significant, at energies around 100 MeV primary and secondary electrons can contribute to the gamma-ray flux at a flux level comparable to the contribution of π^0-decay gamma-rays (see figures and discussion in Appendix B), which would smear out the differences in the derived proton spectra.

To conclude, the detectable fluxes of gamma-rays expected from interactions of CR protons and nuclei with the ambient gas, the lack of other competing gamma-ray production mechanisms in molecular clouds, the effective and (relatively) accurate subtraction of the diffuse gamma-ray background above 1 GeV and (almost) free propagation of high energy CRs through the GMCs, make the latter ideal *detectors* for unbiased studies of the spectral and spatial distributions of CRs in the Local Galaxy at energies above 10 GeV/nucleon. The large exposure time on GMCs accumulated over the several years of LAT continuous monitoring allows a high significant detection of gamma-rays in a broad energy band from a number of GMCs in the Gould Belt, and thus makes feasible the probes of CRs in these objects on a source-by-source basis up to energies of about 1 TeV.

The paper is structured as follows. In Section 2 we describe the GMCs selected for analysis and their characteristics. In Section 3 the results of the analysis of the Fermi

[1] http://fermi.gsfc.nasa.gov/ssc/data/analysis/scitools/aperture_photometry.html

[2] http://fermi.gsfc.nasa.gov/ssc/data/analysis/scitools/ likelihood_tutorial.html

Table 2. Spectral characterists and detection level of the GMC listed in Table 1. The individual χ^2/d.o.f. of the spectral shapes tested is also quoted with the corresponding probabilities in brackets

#	TS	Flux at 3 GeV $[10^{-9}\mathrm{GeV}^{-1}\mathrm{cm}^{-2}\mathrm{s}^{-1}]$	E_b [GeV]	χ^2/d.o.f. (BPL)	χ^2/d.o.f. (KPL)	χ^2/d.o.f. (TPL)
1	4310	9.5 ± 0.8	4.7 ± 2.3	7.5/8 (0.48)	7.8/10 (0.65)	10.4/10 (0.40)
2	258	0.45 ± 0.2	2.4 ± 1.3	3.0/9 (0.96)	5.0/11 (0.93)	3.2/11 (0.99)
3	4031	3.0 ± 0.5	2.0 ± 0.8	8.6/9 (0.47)	12.0/11 (0.36)	14.6/11 (0.2)
4	10068	6.9 ± 0.7	2.3 ± 0.7	11.4/10 (0.33)	24.3/12 (0.02)	20.4/12 (0.06)
5	913	1.2 ± 0.2	3.0 ± 0.7	9/10 (0.53)	28/12 (0.006)	15.5/12 (0.21)
6	8613	9.8 ± 1.0	6.0 ± 3.0	9/10 (0.53)	43/12 (2×10^{-5})	16.5/12 (0.17)
7	1832	1.2 ± 0.2	1.3 ± 0.2	2.2/9 (0.99)	5.31/11 (0.91)	3.8/11 (0.98)
8	1649	2.0 ± 0.5	2.0 ± 0.9	8.0/9 (0.53)	12.7/11 (0.31)	8.6/11 (0.66)
9	4053	3.7 ± 0.3	3.0 ± 0.7	5.5/9 (0.79)	40/11 (4×10^{-5})	15.3/11 (0.17)
10	1405	7.7 ± 0.7	3.6 ± 1.5	11.8/8 (0.16)	94.0/10 (9×10^{-16})	37.0/10 (5×10^{-5})

LAT observations are presented. In Section 4 we derive the CR spectra and fluxes assuming that gamma-rays are produced in interactions of CR protons and nuclei with the ambient gas, and, finally, in Section 5 we discuss the implications of the obtained results.

2. GMCs and the Gould Belt

For our study we have selected ten massive clouds identified in the CO galactic survey of Dame et al. (2001) with the CfA 1.2 m millimetre-wave Telescope (see Table 1). Most of these GMCs belongs or are believe to be associated to the Gould Belt. Only one case, R Coronae Australis (R CrA), lying within the galactic plane on the opposite direction to the Gould Belt, is certain to be unrelated to it. The CO observations provide precise information about the masses and distances to these objects (in Table1). All selected GMCs, except Aquila, are located at high galactic latitude ($|b| > 9°$).

We adopt the estimated distances found in the literature (Dame et al. 1987). In the case of Hercules the distance is derived assuming a flat galactic rotation curve (Burton 1988). Since the calculation of the kinetic energy, necessary to estimate the distance, for nearby clouds is not very accurate, this method might not be appropriated. However, the precision on the distance does not significantly affect our results on the CR flux (see below).

To estimate the total mass contained in the gamma-ray emission region, we used the standard assumption of a linear relationship between the velocity integrated CO intensity, W_{CO} , and the molecular hydrogen column density, N(H2) (Dame et al. 2001) :

$$N(H2)/W_{\mathrm{CO}} = (1.8 \pm 0.3) \times 10^{20}\ \mathrm{cm}^{-2}\mathrm{K}^{-1}\mathrm{km}^{-1}\mathrm{s}^{-1} \quad (1)$$

This equation yields

$$M_{\mathrm{CO}}/M_{\odot} = (1200 \pm 200) S_{\mathrm{CO}} \mathrm{d}^2_{\mathrm{kpc}} \quad (2)$$

where $\mathrm{d}_{\mathrm{kpc}}$ is the distance to the cloud in kpc, and S_{CO} is the CO intensity integrated over the velocity and angular extent of the cloud in K km s^{-1} arcdeg^2. A mean atomic weight of 1.36 is assumed to account for contributions from Helium and heavier elements when deriving Eq. (2). For some clouds our results differ slightly from the estimated masses in the original paper (Dame et al. 1987). This is due to the fact that we used only the central and more homogeneous region of the clouds (to avoid systematic errors due to filaments and uneven edges). Recently, it was argued in a comprehensive review about CO-H2 conversion factor(Bolatto et al. 2013) that a much larger conversion factor of about 4.8×10^{20} $\mathrm{cm}^{-2}\mathrm{K}^{-1}\mathrm{km}^{-1}\mathrm{s}^{-1}$ should be used for the case of Chamaeleon. We adopt this value for Chamaeleon in the calculation below.

It is also important to note (Table 1) that all clouds are extended objects compared to the LAT angular resolution. These large sizes provide an excellent opportunity to explore the clouds morphology with Fermi LAT, excluding uncertainties related to the localisation of the gamma-ray production region. Concerning the impact of uncertainties in M and d in the predicted gamma-ray flux, the expected flux level is proportional to the ratio M/d^2 which depends only on $\sim S_{\mathrm{CO}}$ (Casanova et al. 2010). This minimises the uncertainties providing a high accuracy on the derivation of CR density in the gamma-ray production region. Here we adopted a *standard* conversion factor with an uncertainty of 17% according to Eq. (1). On the other hand, for very dense clouds with large optical depth in CO line, the relation given by Eq. (1) could underestimate the total mass of hydrogen, in some cases perhaps up to by a factor of 2. To account for this we artificially increase our systematic error up to 40%. For future studies it would be important to derived the mass of the clouds based on other molecular lines as well as on the dust measurements. To obtain the spatial template from the CO data, we integrated the CO cube in the velocity dimension to get the total CO intensity (W_{CO}) map of each clouds. The majority of the clouds are located high above the galactic plane, thus the CO distribution is reduced to a single peak, implying a good accuracy when integrating over the whole velocity range.

3. Analysis of the Fermi LAT Data

For the study of the GMCs presented in Table 1 we selected observations with Fermi LAT of the regions around the positions listed in the table integrated over three-years (MET 239557417 - MET 336832558). We used the standard LAT analysis software package(v9r23p1)[3]. To avoid systematic errors due to poor angular resolution and uncertainties in the effective detection area at low energies, we selected only events with energy exceeding 300 MeV. The region-of-interest (ROI) was selected to be a $14° \times 14°$ square centered on the position of each cloud (as determined by Dame et al. 1987). To reduce the effect of the Earth albedo background, we excluded from the analysis the time intervals when the

[3] http://fermi.gsfc.nasa.gov/ssc

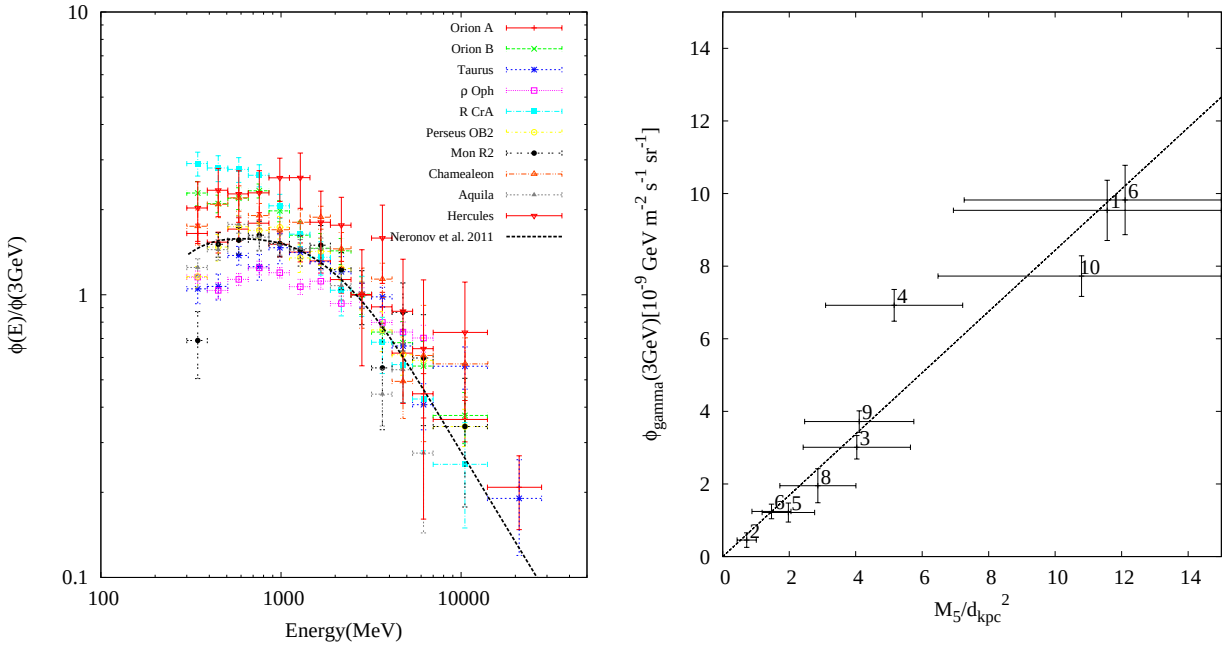

Fig. 1. *Left panel* (a) SED of the gamma-ray emission detected from GMCs in Table 2. For each cloud, the energy spectrum is normalised to its flux at 3 GeV to highlight the differences between the spectral shapes derived from different clouds. The spectrum averaged over the gamma-ray data from all clouds reported by Neronov et al. (2012) is also shown (black curve). *Right panel* (b) Differential gamma-ray flux at 3 GeV versus $M_5/d^2_{\rm kpc}$ (M_5 is the cloud mass in units of $10^5 M_\odot$ and $d_{\rm kpc}$ is distance in units of kpc). The data points are numbered as in Table 2.

Earth was in the field-of-view (specifically when the center of the field-of-view was more than 52° from zenith), as well as the time intervals when parts of the ROI had been observed at zenith angles > 100°. The spectral analysis was performed based on the P7v6 version of post-launch instrument response functions (IRFs). Both the front and back converted photons are selected.

Since the gamma-rays produced in GMCs are already included in the galactic diffuse model provided by the Fermi collaboration[4], it can not be used to evaluate the background. The galactic diffuse emission basically includes the contributions from the inverse Compton (IC) scattering off soft high-energy electrons, and π^0 decay and bremsstrahlung that take place in the H1 and H2 regions.

As shown in Gabici et al. (2007), the contribution of Bremsstrahlung emission in passive clouds is expected to be relevant only below 100 MeV, when the electron to proton ratio is e/p <0.1. Considering the typical estimated ratio of $e/p \sim 0.01$ in the galaxy (Drury 2012), Bremsstrahlung contribution to the gamma-ray emission can be safely neglected when modelling passive clouds (see also Appendix B). To estimate the background, we calculate only the contributions from IC and H1 related emission using GALPROP[5] (Vladimirov et al. 2011), which uses information regarding CR electrons, interstellar radiation field (ISRF) distributions and 21 cm radio data.

To derive the gamma-ray emission from each GMCs we used templates generated from CO data assuming that gamma-rays trace the spatial distribution of the molecular gas. The residual maps after fitting the gamma-ray emission using the templates derived from the clouds do not show any significant excess, proving the good agreement in the location of the gamma-ray emission and the clouds. Point-like sources from the 2FGL catalogue (Abdo et al. 2012) which appear within the ROI were also included in the analysis. We applied *gtlike* and a binned likelihood analysis to obtain spectral features and Test-Statistics (TS) values for each clouds (see Table 2).

All ten GMCs included in this study appeared to be strong gamma-ray emitters; they have been detected at high confidence level with statistical significances TS> 250. To derive their spectral energy distribution (SED) we divided the energy range into logarithmically spaced bands and applied *gtlike* in each of these bands. The results of the spectral analysis are shown in Fig. 1a, where the SEDs are normalised to the corresponding fluxes at 3 GeV in order to highlight the differences on the spectral features of the gamma-rays radiation from different clouds. We also show the spectrum reported by Neronov et al (2012) based on the combined gamma-ray data of all clouds (solid black curve). This curve can be interpreted as the average energy spectrum. However while at high energies the spectra of individual clouds (see Fig.1) are similar this one, below ∼3 GeV the spectra of some clouds deviate substantially.

The main source of systematic errors in the gamma-ray spectrum comes from the uncertainty of the chosen diffuse background templates. In some dense regions, the H1 and CO map may be not sufficient to model the gas distribution. However, as mentioned above, the residual maps show a good agreement between the gamma-ray and CO maps, demonstrating that in this particular region the CO data trace correctly the total gas content involved in the gamma radiation process. On the other hand, the spatial templates of IC generated from GALPROP may be model-dependent.

[4] gal_2yearp7v6_v0.fit and iso_p7v6source.txt, available at http://fermi.gsfc.nasa.gov/ssc/data/access/lat/BackgroundModels.html

[5] http://galprop.stanford.edu/webrun/

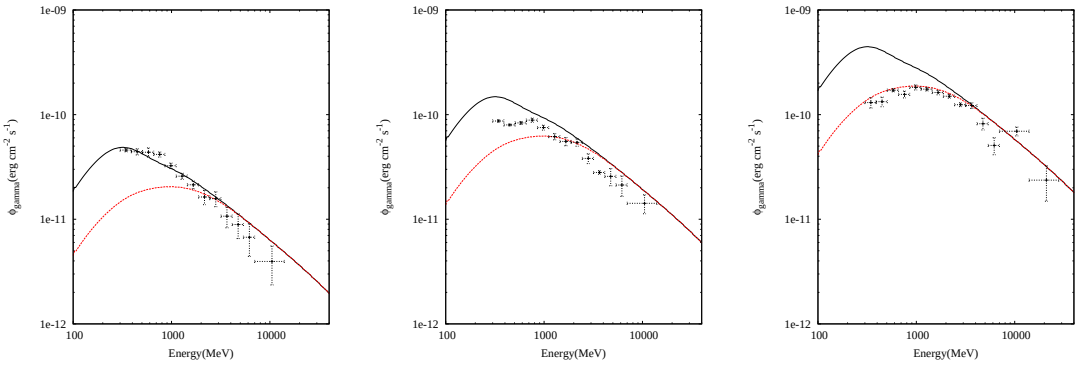

(a) R CrA (b) Orion B (c) Taurus

Fig. 2. SED of three GMCs, R CrA (a), Orion B (b), Taurus (c) as measured by LAT (points). For comparison, the expected gamma-ray flux produced via pp interactions assuming that the CR spectrum inside the clouds is identical to the local one measured by PAMELA (red dashed lines) is also shown. The black solid curves represent the gamma-ray fluxes calculated for a spectrum of CR protons which at high energies coincides with the PAMELA measurements, but towards low energies, down to 1 GeV, continues as a power-law with an index 2.85.

To asses the uncertainties introduced by the IC spatial templates, we modified it attempting to fit the results under different hypothesis (e.g. simple disk and isotropic model). Below 1 GeV, this results in a maximum change on the flux level of 10% for faint sources, while it becomes negligible at high energies. This is the case for clouds away from the galactic plane whereas in the case of Aquila for instance, changes of the diffuse background might alter the derived gamma-ray flux significantly. Considering that the results presented here should be taken with caution for this particular cloud.

Recently, thanks to a significant increase of the effective area at low energy (a factor of 5 at 100 MeV) in the latest version of the Fermi LAT IRFs (Ackermann et al. 2012b), the Fermi LAT collaboration extended their analysis tools down to below 100MeV, crucial to understand the origin of the gamma ray emissions. However, the uncertainties coming from the diffuse background is still severe at low energy. To investigate this we selected one of the clouds (Orion B) with high significance ($TS \sim 4000, E > 300$ MeV) and low background level ($b < -10°$), far from the galactic center as an example to explore the low energy features of the gamma-ray emission. The results and conclusions of this study are summarised in Appendix A.

4. Cosmic rays spectrum

The gamma-ray spectra derived for each GMC from 300 MeV to about 30 GeV show different spectral shapes and flux levels (see Table Fig. 1). Nevertheless the measured gamma-ray flux level, provided that the total gamma-ray emission in each cloud is due only to hadronic interactions of CR with the molecular target, is expected to be proportional to the ratio M/d^2. This general trend is shown in Fig. 1b, in which the differential flux at 3 GeV is plotted versus the M/d^2 ratio. The points are fitted with a simple linear regression which yields a χ^2/d.o.f of 3/9 (Prob=0.93).

Due to the high density of matter in these clouds, we assume that the gamma-ray emission is produced mainly in interactions of galactic CRs and the gas inside the clouds. Under this hypothesis we can derive the CR spectrum and density inside each individual cloud. Recently a convenient formalism has been developed by Villante & Vissani (2009) to derive proton spectrum directly from gamma-ray observations. This method is based on the analytical parametrizations developed by Kelner et al. (2006) for gamma-ray spectra produced at the decays of neutral mesons, the secondary products of proton-proton (pp) interactions. While this parametrization provides good accuracy for protons with energy E$_p$ >100 GeV, it shows some limitations at lower energies due to the approximation of the proton spectrum by a smooth power-law function. To derive then the proton spectrum shape at low energy (down to E$_p$ ≃300 MeV, i. e., the energy threshold for π^0 production) avoiding an a priori assumption of a power-law function to describe it, we chose instead the parametrization developed by Kamae et al. (2005), which formally works for an arbitrary spa trim of protons. It should be noted that this parametrization is less accurate at very high energies (E$_p$ >1 TeV, see e. g. Kachelriess & Ostapchenko 2012), beyond the LAT sensitive energy range.

To investigate the gamma-ray spectrum, specially at low energies, we compare the measured gamma-ray flux in each cloud with the expected gamma-ray emission assuming that the CR spectrum inside the clouds is identical to the one measured by the PAMELA experiment (local CR spectrum hereafter). Such a comparison shows quite different behaviour for different clouds. In some of them, the spectrum is very similar to the one obtained when considering a CR spectrum with an low energy cutoff (likewise the local solar-modulated CR spectrum), whereas some others can be well-fit using a power-law function describing the CR spectrum to energies down to 1 GeV, as it is the generally assumed for the intrinsic spectrum of galactic CRs.

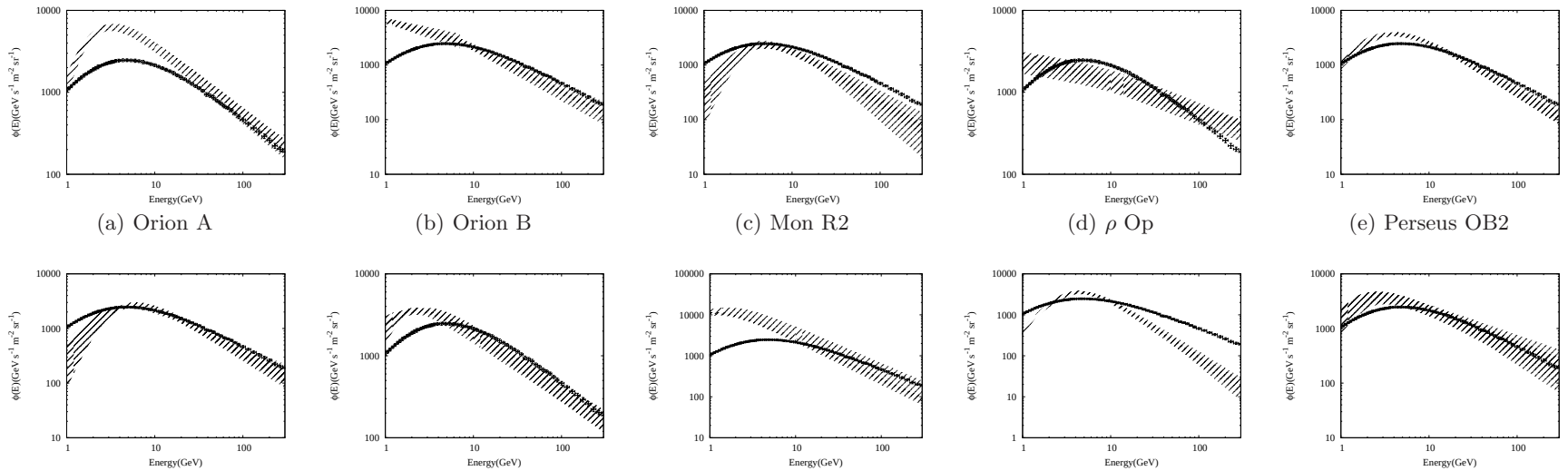

(a) Orion A (b) Orion B (c) Mon R2 (d) ρ Op (e) Perseus OB2

(f) Taurus (g) Chamaeleon (h) R CrA (i) Aquila (j) Hercules

Fig. 3. Energy spectra of CR protons in different clouds derived from the gamma-ray data. It is assumed that the interactions of CR with the ambient gas are fully responsible for the observed gamma-ray fluxes. The shaded regions represent 1σ fits for the proton spectra. For comparison, the measurements of CR protons by PAMELA are also shown (black crosses).

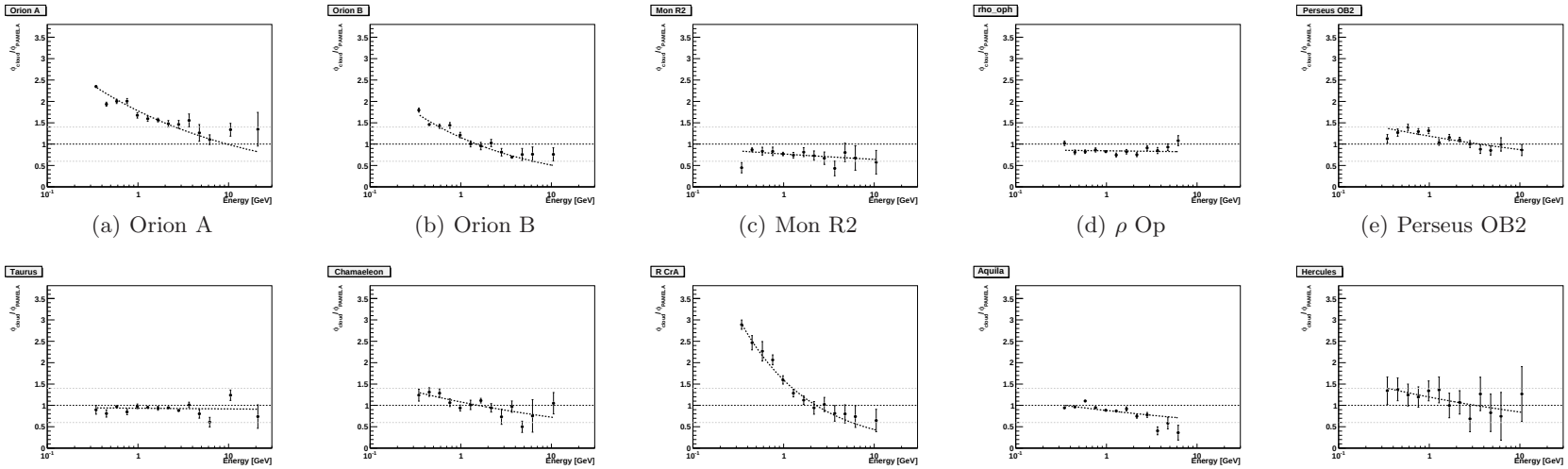

(a) Orion A (b) Orion B (c) Mon R2 (d) ρ Op (e) Perseus OB2

(f) Taurus (g) Chamaeleon (h) R CrA (i) Aquila (j) Hercules

Fig. 4. The ratio of gamma-ray spectra detected by Fermi LAT from different clouds to the calculated gamma-ray spectrum if the CR proton flux in the clouds would be similar to the local CR spectrum measured by PAMELA. The grey lines indicate the allowed range of variations related to uncertainties of total masses of the clouds.

Figure 2 shows three examples in which the measured spectral points of the gamma-ray flux are overlaid with the expected gamma-ray spectrum calculated using the local CR proton spectrum (red dashed line) and a pure power-law proton spectrum (black solid line). While the observed spectrum of R CrA is well described by a gamma-ray spectrum derived from a pure power-law CR spectrum, the two other sources shown, Orion B and Taurus, show some deviation from a pure power-law. The spectrum measured in Taurus shows a very good agreement with the spectrum derived using the local solar-modulated CR spectrum whereas the spectrum for Orion B seems to fall in between the two hypothesis considered, namely, with a harder spectrum at low energy than predicted by local solar-modulated CR spectrum but softer than the one predicted by a pure power-law spectrum.

To obtain the proton spectrum from the gamma-ray observations, we used the statistical approach suggested by Lampton et al. (1976). Three spectral shapes have been assumed for CR protons to fit the gamma-ray data by the spectra of secondary (π^0-decay) gamma-rays: (i) power-law in kinetic energy (KPL):

$$\psi(E) = N\ E^{-\gamma}\ , \tag{3}$$

(ii) power-law in total energy (TPL)

$$\psi(E) = N\ (E_{\rm total})^{-\gamma}\ , \tag{4}$$

(iii) broken power law (BPL)

$$\psi(E) = N\ (\frac{E}{E_b})^{-\gamma_1}[1+(E/E_b)^2]^{\frac{\gamma_1-\gamma_2}{2}}\ , \tag{5}$$

where E and $E_{\rm total} = E + m_{\rm p}c^2$ are the proton kinetic and total energies, respectively; $E_{\rm b}$ corresponds to the break energy, where the index of the power-law distribution smoothly changes from γ_1 to γ_2.

The $\chi^2/d.o.f$ values and associated probabilities to the fit to each spectral template are listed in Table 2. Orion B, Hercules, ρ Oph and R CrA are well-fit by the three representations at the 2σ confidence level. In the other cases, the KPL model is disfavoured by more than 2.5 σ whereas the difference between the TPL and BPL models is not significant. Figure 3 shows the resulted proton spectrum using the BPL hypothesis, where the shaded area accounts for the 1σ error in the fit parameter space. For comparison, the local proton spectrum measured by PAMELA is also shown (crosses).

From the comparison with the local proton spectrum we can conclude:

- The proton spectrum derived from five out of the ten clouds considered, namely Taurus, Persues OB2, Mon R2, Hercules, ρ Oph are well-described by the locally measured proton spectrum by PAMELA.
- The derived proton spectra of Aquila shows a deficit at high energies but it should be noted in this regard that this object is located in the direction of the galactic plane, where the uncertainties in the background model do not allow accurate derivation of the gamma-ray spectrum.
- The last four cases, Orion A, Orion B , Chamaeleon and R CrA should be treated differently. In Orion B and R CrA the proton spectrum is well-described with a KPL function, showing an enhancement of CRs compared to the local CR flux. In Orion A and Chamaeleon, although a BPL function is preferred to describe the proton spectrum, a high enhancement of CRs compared to the local CR flux at low energies is also present. At high energies the spectrum shape is very similar to the one of the local CR. It is important to note that R CrA is the only GMC considered which is not located inside Gould Belt, implying a common behaviour at high-energies independently of the cloud location.

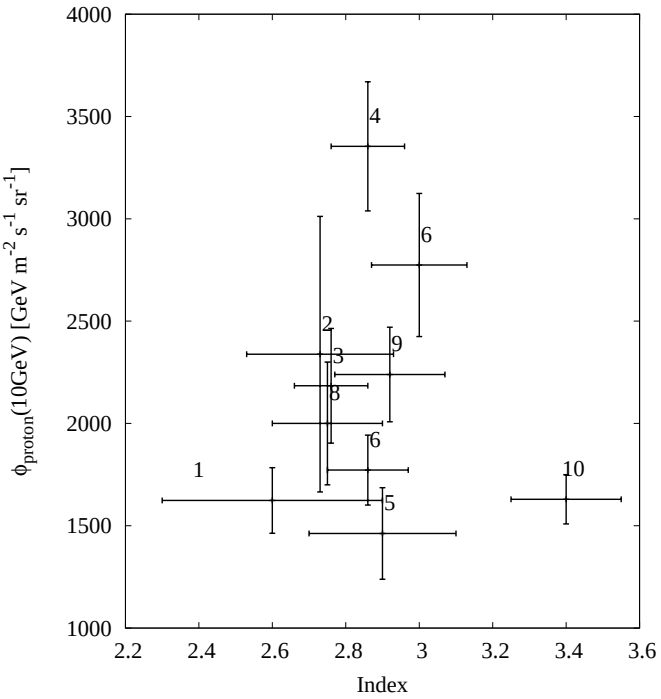

Fig. 5. The power-law index of CR protons above E_b versus differential proton flux at 10 GeV. The data points are numbered as in Table 2.

Figure 5 shows the distribution of the CR spectrum index at high energy ($E > E_{\rm b}$) with respect to the CR flux at 10 GeV. Most of the spectral indices found are compatible ($<2\sigma$) with the CR *sea* spectral index of 2.8. The only exception is the one corresponding to Aquila (3σ deviation) which suffers from background subtraction as discussed above. The index for ρ Oph is also a little smaller (2.6 ± 0.3) than 2.8. However, the SED of ρ Oph only extend to $\approx$7 GeV, preventing a good determination of the spectral index at high energies.

To explore further the impact of deviation of the proton spectra in the clouds from the locally measured CR flux, we calculated for each cloud the ratio of the measured gamma-ray flux to the expected one under the hypothesis that the CR flux inside the cloud is identical to the local CR flux. These results are shown in Fig. 4. The indicated errors bars account for both statistics and systematics errors (grey dashed lines). The effects discussed above can also be observed here: the SED of Orion B, Orion A, Chamaeleon and R CrA show different spectral features compared to the expected gamma-ray spectrum produced by the local CRs at low energies. The same effect is observed in R CrA (not associated to the Gould Belt) where the CR spectrum shows a clear deviation from the predicted one.

5. Summary

Giant molecular clouds can serve as unique *barometers* for determination of the pressure (energy density) of CRs throughout the Galaxy via their characteristic high energy gamma-ray emission produced in CR interactions with the dense ambient gas. A similar information can be found also by analyzing the diffuse gamma-ray background of the galactic disk in different directions. However in the case of the diffuse gamma-ray background, the extracted CR spectrum is averaged over huge distances on ≥ 10 kpc scales, while the information about CRs derived from individual clouds is localized within tens of parsecs.

The high quality data obtained by Fermi LAT provide adequate observational material for such studies. In this paper we present the result of our analysis of three-year observations of ten GMCs detected by Fermi LAT. At high energies, the analysis of gamma-ray emission from all GMCs, except for Aquila and ρ Oph, which have limited statistics or/and suffer from large uncertainties in the estimates of the background, show that the CR proton spectra above a few GeV are well-described by a power-law function with an index of $\Gamma = 2.85$. This is slightly softer than previous measurements (see e. g. Boezio et al. 1999) but agrees very well with the CR proton spectral index reported by the PAMELA collaboration (Adriani et al. 2011). Remarkably, the derived absolute fluxes of CRs are also in good agreement with the direct measurements of local CRs. It should be noted, however, that this conclusion is based on the estimates of the clouds mass based on CO observations which contain rather large, up to 50 % uncertainties. Moreover, it has been recently argued (see i.e. Planck Collaboration et al. 2011 and references therein) that the gas is not adequately traced by CO measurements, and the total mass could be underestimated up to by a factor of two. Whether this claim concerns the specific clouds used in this paper, and if yes, then to which extent, this is a question which will be clarified, hopefully soon. Meanwhile, we should worn that any substantial revision of masses of the clouds in the Gould Belt, which could be only towards the increase of the mass estimates would unavoidably lead to a surprising conclusion, namely it would lead to the reduction of the estimates of the CR energy flux well below the level locally measured by Pamela. This seems rather unlikely, but cannot be fully excluded. The prime importance of this question for the origin of galactic CRs apparently initiate new model-independent measurements of masses of clouds in Gould Belt.

At low energies, typically below 10 GeV, we should expect a strong suppression of the flux of local CRs due to modulation while propagation through the solar system. This effect can be seen in the spectrum reported by the Pamela collaboration. The *recovery* of the initial (unmodulated) CR spectrum at low energies is a quite difficult task and depends on theoretical (model) assumptions. This increases the importance of deriving the spectra of galactic CRs from gamma-ray observations of *passive* clouds. However, propagation effects might have a strong impact on the penetration of low energy CRs into the GMCs, and therefore also in the spectrum of secondary gamma-rays. The gamma-ray spectra of six out of ten GMCs used in the present study (see Fig.5), do not significantly deviate from the expected one if the CR spectra in these clouds would be similar to the locally measured CR spectrum. In this regard it should be noted that the suppression of the spectrum of local CRs is unavoidable due to the solar modulation. Generally, we should expect non-negligible modulation of the spectrum of galactic CRs at their entrance into the complexes of dense molecular clouds and star formation regions as well. However, it is suspicious that the modulation of galactic CRs in such different environments (the solar system and massive molecular clouds) could have the same effect on the deformation of the spectrum of galactic CRs. At first glance, a possible explanation of this coincidence could be that the modulation effects are negligible and the local CRs spectrum measured by PAMELA is the same as the galactic CR spectrum not only at high energies but also below 10 GeV. However, since there could be little doubt in significant modulation of CRs in the solar system, it is more likely that the similarity of the CR spectra in clouds and the local CR spectrum measured by Pamela at low energies does not have a deep physical reasoning, especially given that only in two cases, ρ Oph and Taurus, the CR proton spectra mimic the Pamela spectrum. Moreover, the good representation of the gamma-ray spectra of Orion A, Orion B, Chamaeleon and R CrA (see Fig. 3) by interactions of CRs with pure power-law spectra of parent protons down to 1 to 3 GeV, supports the interpretation of the diversity of spectral shapes of CRs in different clouds below 10 GeV as a result of propagation effect. In this regard, the gamma-ray spectra of these four clouds indicate a small effect of particle propagation in these clouds, therefore the power-law spectra of protons derived in these clouds could be taken as representatives for the *sea* of galactic CRs. The energy density corresponding to this spectrum (which continuous as power-law in kinetic energy with index $\Gamma \approx 2.85$ from energies ≥ 100 GeV down to 2 GeV) is ~ 0.65 eV/cm^3, while for the local CR spectrum measured by Pamela the density is a factor of 4 less.

Finally, combining this spectrum with the well established (in this energy interval) energy-dependent time of escape of CRs from the Galaxy, $\tau(E) \propto E^{-\delta}$ with $\delta \approx 0.5 - 0.6$, implies a source (acceleration) of galactic CRs below 100 GeV with spectral index close to $E^{-2.3}$, which is somewhat steeper than one would expect from the standard diffusive shock acceleration theory.

The determination of the low energy galactic CR spectrum has important implications on various astrophysical issues, such as ionisation and heating of ISM by low energy CRs and contribution to the overall pressure in the ISM. It also has an impact on the determination of the diffuse gamma-ray background, which is crucial for correct interpretation of the high energy observations. Further studies of processes with involvement of propagation and gamma-ray production by CRs in massive molecular clouds are needed. In particular, the continuation of the analysis of the Fermi LAT data based on more time exposure of these objects, is important for the search for smaller differences in the gamma-ray spectra.

Appendix A: Low energy gamma-ray emission of Orion B

To derive the SED down to 100 MeV from Orion B, we use the same analysis method described in the text, modifying the energy cut to include low-energy photons. The derived gamma-ray flux is shown in Fig.A.1. The differential spectrum in the low energy bins shows a flattening

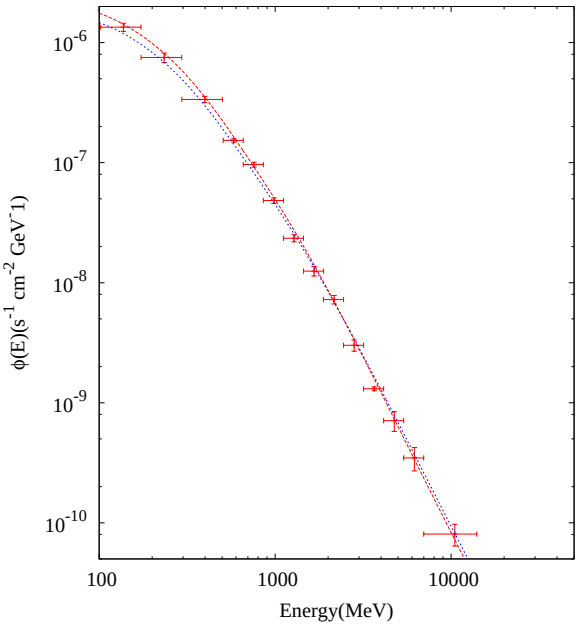

Fig. A.1. The differential spectrum for Orion B including the low energy data points down to 100 MeV. The solid curve was calculated using the BPL proton spectrum described in the text with $E_b = 2$ GeV, $\gamma_1 = 1.0$ and $\gamma_2 = 2.86$, while the dotted curve using TPL model with $\gamma = 2.90$

.

which most likely corresponds to the distinct feature expected in the pion-decay spectrum. This is demonstrated by the theoretical spectra of gamma-rays which are also shown in Fig.A.1. These curves are obtained for two type of proton spectra: BPL and TPL (as described in the text). For the BPL hypothesis we adopt $E_b = 2$ GeV, $\gamma_1 = 1.0$ and $\gamma_2 = 2.85$ while for TPL model the index was set to be $\gamma = 2.90$. These indices are close to that observed by PAMELA (Adriani et al. 2011). The results are shown in solid and dotted curves in Fig.A.1, respectively. Note that the gamma-ray fluxes in the entire energy band, including the low energy part, can be fitted quite well by pure π^0 contributions. Also we note that there is not any need to assume a break in the CR spectrum down to 1-2 GeV. However, it should be kept in mind the possible contribution of the primary and secondary electrons which at 100 MeV can be as large as 50 %. If so, a break in the proton spectrum at energy somewhat higher than 2 GeV might be needed. Also, at low energies the uncertainty in the diffuse background could be quite large and this issue should be investigated carefully before we draw any conclusion concerning the proton spectrum around a few GeV.

Appendix B: Gamma-ray production mechanism in molecular clouds

Gamma-rays are produced in molecular clouds through different radiation mechanism, namely in proton-proton collision via production and decay of neutral pions, due to electron Bremsstrahlung, as well as inverse Compton (IC) scattering of the primary and secondary electrons. To show the contributions from different mechanism, we consider a molecular cloud with a mass of $10^5 M_\odot$ located 1 kpc away from us. The proton and primary electron spectrum measured by PAMELA (Adriani et al. 2011) are used to calculate the gamma ray spectrum. We show the gamma-ray spectra for CR distributions extrapolated from high energies as a pure power-law down to low energies. For the spectrum of secondary electrons, we take into account the radiative energy losses, but assume that electrons do not escape the cloud. This implies that the corresponding fluxes of the secondary gamma-rays should be treated as upper limits. It is shown in FigB.1 that at all energies above 100 MeV the pion decay dominates over the contributions from the electrons. While the IC fluxes are negligible, around 100 MeV the gamma-ray flux from Bremsstrahlung of primary electrons becomes significant, approximately 25% (of the π^0-decay gamma-ray flux) for the locally measured electron spectrum and almost 100% for the CR spectrum extrapolated from high energies as a pure power-law down to low energies. The electron spectrum in the interstellar medium below 1 GeV derived from the radio synchrotron measurements is between these two approximations, therefore the curves shown in Fig.B.1 can be considered as the lower and upper limits of the contribution of Bremsstrahlung of primary electrons. The Bremsstrahlung of secondary electrons may be important as well (up to about 50% at 100MeV), however in the case of effective escape of these particles from the cloud their contribution would be dramatically reduced. Finally we note the difference of gamma-ray spectra produced at energies a few GeV by the Pamela-type and pure power-law proton spectra. Since the spectrum measured by Pamela is strongly modulated in the Solar system, the proton spectrum with power-law shape extending down to low energies seems more realistic for the galactic CRs. Nevertheless, if the entrance of low-energy galactic CRs into the cloud is prevented, the gamma-ray fluxes at low energies will be suppressed. Thus, the two curves corresponding to π^0 gamma-rays in Fig.B.1 should be considered as lower and upper limits.

References

Abdo et al. 2012, Astrophys.J.Suppl., 199, 31
Achermann, M. et al. 2012
Ackermann, M., Ajello, M., Allafort, A., et al. 2012a, Astrophys.J., 756, 4
Ackermann, M. et al. 2012b, Astrophys.J.Suppl., 203, 4
Adriani, O., Barbarino, G. C., Bazilevskaya, G. A., et al. 2013, ApJ, 765, 91
Adriani, O. et al. 2011, Science, 332, 69
Aharonian, F. A. 2001, Space Science Reviews, 99, 187
Atwood, W. et al. 2009, Astrophys.J., 697, 1071
Bolatto, A. D., Wolfire, M., & Leroy, A. K. 2013, ArXiv e-prints,ArXiv:1301.3498
Burton, W. B. 1988, The structure of our Galaxy derived from observations of neutral hydrogen, ed. K. I. Kellermann & G. L. Verschuur, 295–358
Casanova, S., Aharonian, F. A., Fukui, Y., et al. 2010, PASJ, 62, 769
Dame, T. M., Hartmann, D., & Thaddeus, P. 2001, ApJ, 547, 792
Dame, T. M., Ungerechts, H., Cohen, R. S., et al. 1987, ApJ, 322, 706
Drury, L. O. 2012, Astropart.Phys., 39-40, 52
Gabici, S., Aharonian, F. A., & Blasi, P. 2007, Ap&SS, 309, 365
Grenier, I. A., Casandjian, J.-M., & Terrier, R. 2005, Science, 307, 1292
Kamae, T., Abe, T., & Koi, T. 2005, ApJ, 620, 244
Kelner, S., Aharonian, F. A., & Bugayov, V. 2006, Phys.Rev., D74, 034018
Lampton, M., Margon, B., & Bowyer, S. 1976, ApJ, 208, 177
Montmerle, T. 1979, ApJ, 231, 95
Neronov, A., Semikoz, D., & Taylor, A. 2012, Phys.Rev.Lett., 108, 051105

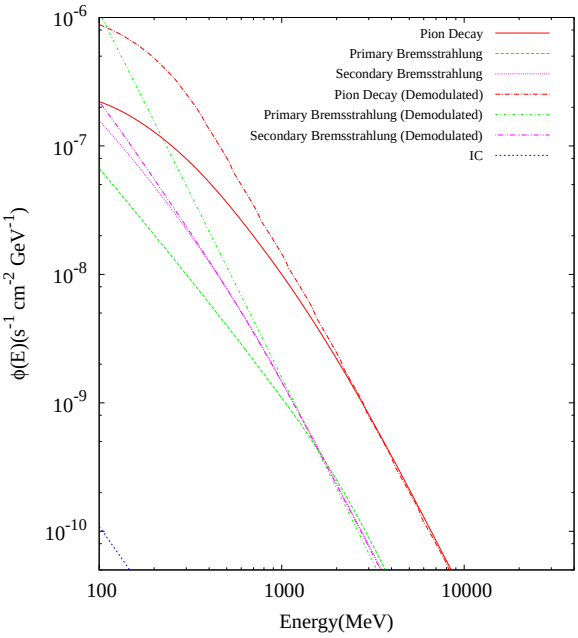

Fig. B.1. The differential spectrum of gamma rays produced in molecular clouds by different mechanisms. Both the PAMELA measurement and a pure power law function extrapolated to low energies (demodulated) are considered.

.

Pedaletti, G., Torres, D. F., Gabici, S., et al. 2013, A&A, 550, A123
Perrot, C. A. & Grenier, I. A. 2003, A&A, 404, 519
Planck Collaboration, Ade, P. A. R., Aghanim, N., et al. 2011, A&A, 536, A19
Villante, F. L. & Vissani, F. 2009, Nuclear Physics B Proceedings Supplements, 188, 261
Vladimirov, A. E., Digel, S. W., Jóhannesson, G., et al. 2011, Computer Physics Communications, 182, 1156